Migration-Driven Instability in the Chlorite−Tetrathionate Reaction

Zsanett Viranyi, Dezsó Horváth, and Ágota Tóth*

Department of Physical Chemistry, University of Szeged, P.O. Box 105, Szeged, H-6701 Hungary

Received: October 24, 2005; In Final Form: January 20, 2006

We have studied the lateral stability of planar reaction−diffusion fronts in an autocatalytic reaction between aqueous ions in an externally imposed electric field. In our experiments, migration drives the pattern formation leading to cellular structures where the sufficiently greater migrational flux of the reactant with respect to that of the autocatalyst is the driving force. The difference in electric field strength between the two sides of the thin reaction front results from the significant increase in conductivity during the reaction. The results of the theoretical analysis based on the empirical rate-law model of the reaction reproduce the behavior observed experimentally.

1. Introduction

A chemical front may be triggered in an unstirred reactant mixture of an autocatalytic reaction by supplying the autocatalyst in a confined space. The initiated reaction front that propagates through the medium and converts the reactants into products is the result of the coupling between the autocatalytic reaction kinetics and transport processes, among which diffusion is the most common.[1−3] In solutions where convection is negligible, the geometry of the reaction front reflects that of the local initiation: in a thin layer, a point source results in a circular front, whereas a straight line leads to a planar front. Even though the reactants are homogeneously distributed ahead of the front, concentration gradients transverse to the direction of propagation may arise from microscopic noise.[4] This lateral instability of reaction−diffusion fronts has been observed experimentally[5−8] and studied thoroughly theoretically.[9−14] The necessary requirement for the instability apart from the sufficiently strong autocatalysis is the slower diffusion rate of the autocatalyst at the front with respect to that of the reactant. This has been achieved experimentally by decreasing the concentration of free autocatalyst produced behind the front, and hence its gradient across the thin reaction zone, via reversible binding into an immobile compound[5−8] or with an appropriately oriented constant external electric field parallel to the direction of front propagation in an ionic reaction.[12,13,15] It is also known that an external electric field may further change the front characteristics and even the stoichiometry of the underlying chemistry and, hence, has a profound effect on the pattern formation.[16−19]

The chlorite oxidation of tetrathionate in slight chlorite excess[20]

$$7ClO_2^- + 2S_4O_6^{2-} + 6H_2O = 7Cl^- + 8SO_4^{2-} + 12H^+ \quad (1)$$

with an empirical rate law in the form of $R = k_r[ClO_2^-][S_4O_6^{2-}][H^+]^2$ is an acid-catalyzed reaction producing large amount of ions in the course of the reaction. It has been shown that the empirical rate-law can be used to describe the spatiotemporal pattern formation under the experimental conditions applied.[21,22] The spatiotemporal pattern formation has been extensively studied both in closed[6,23] and open systems.[24,25] Lateral instability has been observed in this reaction where the selective immobilization of the autocatalyst hydrogen ion has been achieved by binding it to methacrylate groups reversibly in a cross-linked polymeric hydrogel used as a convection-free medium.[6,15] In an earlier experimental study, we have also shown that migrational flux at the front imposed by an inhomogeneous electric field may shift the onset of instability in the opposite way with respect to the effect of diffusive flux driving the pattern formation.[26]

In this work, we study the reaction above but in the absence of binding groups and introduce an inhomogeneous electric field controlled by a constant current density parallel to the direction of front propagation. We first show experimentally that lateral instability of planar fronts leading to the formation of cellular patterns may be driven exclusively by the difference in the migrational flux of the reactants and the autocatalyst. It is demonstrated in a system where the autocatalyst hydrogen ions diffuse significantly faster than the reactants, which represents a strong stabilization of planar fronts in the absence of electric field. We then carry out a thorough theoretical analysis of the model of the reaction under the experimental conditions and reproduce the important experimental observations.

2. Experimental Study

Throughout the experiments, analytical grade chemicals were used (Reanal, Sigma, Aldrich) except sodium chlorite which was recrystallized following the recipe from our previous work,[21] and the salt had at least 97% purity. The experiments were carried out at room temperature, 23 ± 1 °C. The thin gel used as a convection-free medium was made of cross-linked polyacrylamide and prepared a day prior to the experiments. Having been rinsed in water several times, a rectangular piece of gel (9.2 cm × 6.5 cm × 1.0 mm) was soaked in the reactant solution with composition given in Table 1 for 15−30 min to ensure the homogeneous distribution of ions. Excess water was carefully wiped off from the surface of the gel, which was then laid between two Plexiglas plates. Thin strips of gel soaked in pure water were also positioned around the rectangular gel before sealing the gap to avoid evaporation that might introduce undesired boundary effects along the edges. One of the plates was fitted with a pair of parallel platinum wires (0.1 mm in

* To whom correspondence should be addressed. E-mail: atoth@chem.u-szeged.hu.

10.1021/jp056084l CCC: $33.50
Published on Web 02/24/2006

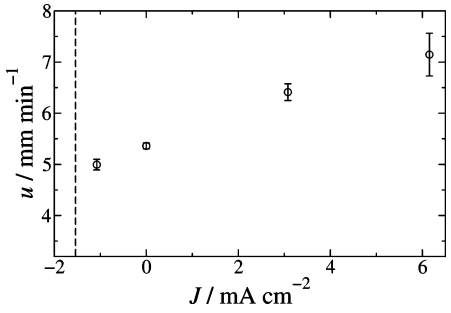

Figure 1. Velocity of propagation of autocatalytic reaction fronts as a function of current density. Dashed vertical line represents the threshold current density beyond which no sustained reaction front is observed. Reactant concentrations are listed in Table 1.

TABLE 1: Composition of Reactant Solution

$[K_2S_4O_6]$/mM	5.0
$[NaClO_2]$/mM	20.0
[NaOH]/mM	1.0
[Congo red]/mM	0.574

diameter) 7.8 cm apart, which was used for both initiating the chemical fronts and then setting up the appropriate electric field in the direction of propagation. A short (2−3 s) electrolysis at 3 V potential difference produced the small amount of hydrogen ions at the anode necessary to initiate an autocatalytic acidity front. A constant current drawn from a galvanostat (Electroflex EF1307) from −4 to +4 mA was maintained, yielding a current density J in the range of −6.5 to +6.5 mA/cm^2. The fronts were monitored with a monochrome CCD camera connected to a computer-driven MVDelta imaging board using an appropriate filter to enhance visualization. Images of 768 × 576 pixels were stored at intervals of 5−60 s as soon as the front was sufficiently far from the electrodes in order to avoid side effects from the electrolysis products. The conductance of the gel was measured with a conductivity meter (Radelkis OK-112) before and after an experiment with the platinum electrodes still in place.

3. Experimental Results

In the absence of an external electric field, the chlorite−tetrathionate reaction exhibits an autocatalytic front that travels at a constant velocity through the gelled medium. When a negative electric field is applied, i.e., the positive electrode is positioned ahead of the front, the velocity of front propagation decreases (see Figure 1). Reaction fronts maintain the geometry of the platinum electrode used for initiation; therefore, planar fronts are stable to the ever present microscopic disturbances as they travel into the homogeneous reactant zone similarly to those in the absence of an external electric field as shown in Figure 2a. Beyond a threshold current density ($J_{lim} \approx -1.5$ mA/cm^2), however, no reaction fronts with constant velocity of propagation can be observed.

In a positive field, i.e., when the negative electrode is placed ahead of the front, the velocity of propagation increases due to the enhanced mixing of the reactant tetrathionate and chlorite and the autocatalyst hydrogen ion resulting from their migration under the imposed external field. Above a critical current density ($J_{cr} \approx 2.6$ mA/cm^2), the initially planar reaction fronts become unstable and cellular fronts develop as shown in Figure 2b. The observed instability can be best characterized by constructing the dispersion curves from a series of images as an initially planar front loses its symmetry. The amplitude of the Fourier

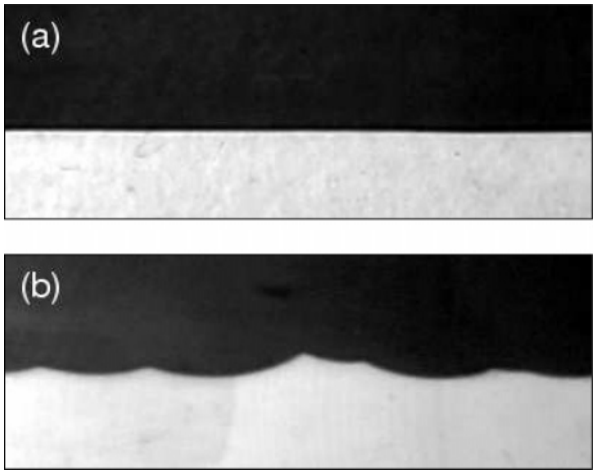

Figure 2. Image of a front at $J = -1.08$ mA/cm^2 (a) and $J = +6.15$ mA/cm^2 (b). Light regions correspond to the reactant and dark regions to the product solution. Field view is 3.64 cm × 1.36 cm. Reactant concentrations are listed in Table 1.

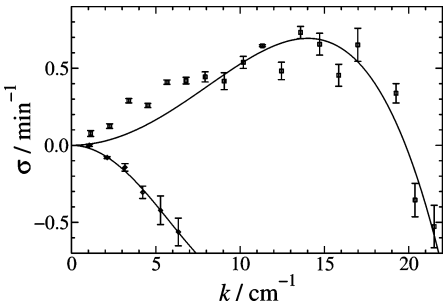

Figure 3. Experimentally determined dispersion curves of observed fronts at $J = -1.08$ mA/cm^2 (●) and $J = +6.15$ mA/cm^2 (■). Reactant concentrations are listed in Table 1.

modes present in the front profiles exponentially decrease or increase depending on their spatial wavenumber. Figure 3 presents two example cases: for $J = -1.08$ mA/cm^2, all modes have negative growth rate coefficients (σ); therefore, perturbations decay in time leading to a stable planar reaction front. At $J = 6.15$ mA/cm^2, however, a range of wavenumbers with positive growth rate coefficients exists, and hence, these modes have amplitudes increasing in time. An initially planar front loses its symmetry, and a cellular pattern develops in the front profile transverse to the direction of propagation. The average wavelength of cells lies in the vicinity of that of the most unstable mode in the dispersion curve, indicating that the latter drives the initial stage of the pattern formation.

4. Modeling Study

The reaction−diffusion−migration system with eq 1 in an electric field can be described by considering the balance equations for the components as

$$\frac{\partial C_i}{\partial t} = D_i \nabla^2 C_i + \frac{z_i F D_i}{RT} \nabla (C_i \nabla \Psi) + \nu_i R \qquad (2)$$

where C_i represents the concentration of $S_4O_6^{2-}$, ClO_2^-, H^+, Cl^-, SO_4^{2-}, and K^+ respectively. For simplification, only a single type of counterion is assumed, and the empirical rate law based on the initial rates as $R = k_r C_1 C_2 C_3^2$ is taken to be valid in the entire course of the reaction. We also assume that small aqueous ions have the same diffusion coefficient with the exception of the autocatalyst hydrogen ion. The complete description includes the charge balance as

$$\frac{\partial Q}{\partial t} = \sum_{i=1}^{6}\left(z_i F D_i \nabla^2 C_i + \frac{z_i^2 F^2 D_i}{RT}\nabla(C_i \nabla \Psi)\right) = 0 \qquad (3)$$

For the analysis we introduce dimensionless concentrations $c_i = C_i/C_{1,0}$ with respect to the initial concentration of the limiting reactant tetrathionate ion ($C_{1,0}$), dimensionless time scale $\tau = k_r C_{1,0}{}^3 t$, and dimensionless length scales with $\xi = x(k_r C_{1,0}{}^3/D_1)^{1/2}$ in the direction of front propagation and η, analogously to ξ, perpendicular to that, redefining $\nabla = (\partial/\partial\xi,\ \partial/\partial\eta)^T$. The dimensionless potential is scaled as $\psi = \Psi F/(RT)$, and the relative diffusivities are defined by $\delta_i = D_i/D_1$, yielding $\delta_i = 1$ for $i \neq 3$. The governing equations now have the form

$$\frac{\partial c_i}{\partial \tau} = \delta_i \nabla^2 c_i + z_i \delta_i \nabla(c_i \nabla\psi) + \nu_i c_1 c_2 c_3{}^2 \qquad (4)$$

$$0 = \sum_{i=1}^{6}(z_i \delta_i \nabla^2 c_i + z_i{}^2 \delta_i \nabla(c_i \nabla\psi)) \qquad (5)$$

augmented with the appropriate boundary conditions: zero gradients for both concentrations and potential perpendicular to the direction of propagation, and zero gradients for the concentrations far ahead and behind the front where the potential gradient is determined by the current density (J) as

$$\frac{\partial \psi}{\partial \xi} = \frac{-j}{\sum_{i=1}^{6} z_i^2 \delta_i c_i} \qquad (6)$$

with the dimensionless parameter being defined as $j = J/[F(k_r C_{1,0}{}^5 D_1)^{1/2}]$.

For the stability analysis, we first consider a planar front traveling along the ξ-direction, i.e., all gradients with respect to η vanish in eqs 4 and 5, and introduce a moving coordinate $\zeta = \xi - u\tau$, where u is the velocity of front propagation. The resultant

$$0 = \delta_i \frac{d^2 c_i}{d\zeta^2} + u\frac{dc_i}{d\zeta} + z_i \delta_i\left(\frac{dc_i}{d\zeta}\frac{d\psi}{d\zeta} + c_i\frac{d^2\psi}{d\zeta^2}\right) + \nu_i r \qquad (7)$$

$$0 = \sum_{i=1}^{6}\left[z_i \delta_i \frac{d^2 c_i}{d\zeta^2} + z_i{}^2 \delta_i\left(\frac{dc_i}{d\zeta}\frac{d\psi}{d\zeta} + c_i\frac{d^2\psi}{d\zeta^2}\right)\right] \qquad (8)$$

with $r = c_1 c_2 c_3{}^2$ represents a two-point boundary value problem. The boundary condition far ahead of the front at $\zeta \rightarrow +\infty$ is given by the composition of the initial reaction mixture as $c_1 = 1$, $c_2 = 4$, $c_3 = c_4 = c_5 = 0$, and $c_6 = 6$, whereas that far behind the front at $\zeta \rightarrow -\infty$ can be determined from the integral of eq 7 between the limits. Since the limiting tetrathionate is completely consumed in the course of the reaction, i.e., $c_1 = 0$, the integral for the first component yields an expression for the source strength of the reaction as

$$\int_{-\infty}^{+\infty} r\, d\zeta = \frac{u}{2} - \frac{d\psi}{d\zeta}\Big|_{+\infty} \qquad (9)$$

The rest of the integrals with the formula above provides a set of equations for c_2, c_3, c_4, and c_5 at $\zeta \rightarrow -\infty$. The concentration of the counterion (c_6) is finally obtained from the charge balance.

To analyze the stability of the planar front profile, i.e., the solution of eqs 7 and 8, we introduce a small perturbation transverse to the direction of propagation in the form of

$$c_i = c_{0,i}(\zeta) + \sum_{k=1}^{\infty} c_{1,i,k}(\zeta)\Phi(\eta,\tau) = c_{0,i}(\zeta) + \sum_{k=1}^{\infty} c_{1,i,k}(\zeta) e^{\omega\tau + ik\eta} \qquad (10)$$

$$\psi = \psi_0(\zeta) + \sum_{k=1}^{\infty} \psi_{1,k}(\zeta)\Phi(\eta,\tau) = \psi_0(\zeta) + \sum_{k=1}^{\infty} \psi_{1,k}(\zeta) e^{\omega\tau + ik\eta} \qquad (11)$$

where $c_{0,i}$ and ψ_0 represent the solutions to eqs 7 and 8, whereas k is the wavenumber associated with the spatial perturbation. The substitution of eqs 10 and 11 into eqs 4 and 5 together with the introduction of the moving coordinate system leads to

$$\omega c_{1,i,k} = \delta_i \frac{d^2 c_{1,i,k}}{d\zeta^2} + u\frac{dc_{1,i,k}}{d\zeta} + z_i\delta_i\left(\frac{dc_{0,i}}{d\zeta}\frac{d\psi_{1,k}}{d\zeta} + \frac{dc_{1,i,k}}{d\zeta}\frac{d\psi_0}{d\zeta} + c_{1,i,k}\frac{d^2\psi_0}{d\zeta^2} + c_{0,i}\frac{d^2\psi_{1,k}}{d\zeta^2} - k^2 c_{0,i}\psi_{1,k}\right) - \delta_i k^2 c_{1,i,k} + \nu_i J_k \qquad (12)$$

$$0 = \sum_{i=1}^{6}\left[z_i\delta_i\left(\frac{d^2 c_{1,i,k}}{d\zeta^2} - k^2 c_{1,i,k}\right) + z_i{}^2\delta_i\left(\frac{dc_{0,i}}{d\zeta}\frac{d\psi_{1,k}}{d\zeta} + \frac{dc_{1,i,k}}{d\zeta}\frac{d\psi_0}{d\zeta} + c_{1,i,k}\frac{d^2\psi_0}{d\zeta^2} + c_{0,i}\frac{d^2\psi_{1,k}}{d\zeta^2} - k^2 c_{0,i}\psi_{1,k}\right)\right] \qquad (13)$$

for the terms linear in Φ, where $J_k = \sum_{i=1}^{6} (\partial r/\partial c_i)_0\, c_{1,i,k}$. The planar front becomes unstable if the temporal eigenvalue ω takes a positive value for some k, in which case spatial perturbations with wavenumbers having positive ω grow in time. The phenomenon may be best characterized with the construction of the dispersion curve $\omega = \mathcal{F}(k)$, which can be calculated without knowing the first-order perturbation ($c_{1,i,k}$ and $\psi_{1,k}$) because eqs 12 and 13 may be rewritten in matrix form as

$$\omega\begin{pmatrix} 1 & \cdots & 0 & 0 \\ \vdots & \ddots & \vdots & \vdots \\ 0 & \cdots & 1 & 0 \\ 0 & \cdots & 0 & 0 \end{pmatrix}\begin{pmatrix} c_{1,1,k} \\ \vdots \\ c_{1,6,k} \\ \psi_{1,k} \end{pmatrix} = \mathbf{M}\begin{pmatrix} c_{1,1,k} \\ \vdots \\ c_{1,6,k} \\ \psi_{1,k} \end{pmatrix} \qquad (14)$$

which represents a generalized eigenvalue problem with the matrix $\mathbf{M}$ only depending on $c_{0,i}$, ψ_0, and k.

For the two-dimensional calculations, eqs 4 and 5 have been solved on a rectangular grid of 201 × 401 points with $h = 0.2$ spacing using the standard nine-point formula for the Laplacian and an explicit Euler-method with $\Delta\tau = 10^{-3}$. After each iteration step, the potential has been recalculated by applying a relaxation method on eq 5 with routines similar to those for solving eq 4 itself. For initial conditions, a local perturbation of the planar front is introduced by randomly displacing the rows one grid in the direction of propagation. During the integrations, the entire grid is continuously shifted forward to keep the reaction front in the center in order to avoid the artificial depletion of reactants through migration because of the potential field close to the boundary.

A relaxation method is applied for the planar front profiles of eqs 7 and 8 on 501 grid points with $h = 0.05$ spacing using the standard three-point formula for the Laplacian and the forward difference formula for the first derivatives. The potential itself is not considered as a variable in the one-dimensional calculations because the discretization of eq 8 leads to a linear

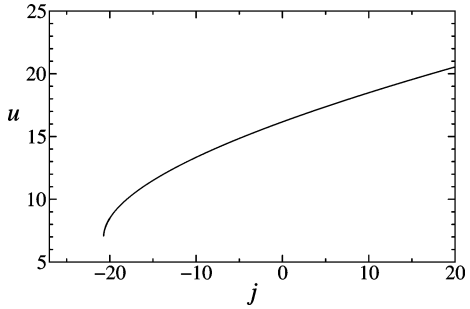

Figure 4. Velocity of propagation of calculated planar fronts as a function of current density. Parameter value used for calculations: $\delta_3 = 2$.

system for ψ with a tridiagonal matrix. Hence, the potential can be readily calculated from the concentrations. The CVODE package[27] is used for the numerical integrations of eq 7, during which the front velocity is constantly adjusted to obtain a value consistent with the criterion in eq 9 within a preset limit of 10^{-7}. For the boundary conditions, exponential concentration profiles are taken where the exponents correspond to the eigenvalues associated with the heteroclinic orbit connecting the two boundary conditions that appear as steady states in the phase space (c_1, ..., c_5, $dc_1/d\zeta$, ..., $dc_5/d\zeta$).

The discretized version of eq 14 yields a regular matrix **M** depending on only the planar front solution and the spatial wavenumber k of the perturbation. Having calculated the solution to eqs 7 and 8, we can construct **M**, which is a 3507 × 3507 square matrix for the 501 grid points. We have used the DGGEV routine from the LAPACK package[28] to find the eigenvalues, among which the ones with the largest real part determine the stability of the planar solution to perturbation with spatial wavenumber k. The dispersion curve is constructed by repeating the procedure and selecting the appropriate distinct eigenvalues for a range of wavenumbers.

5. Numerical Results

In a negative electric field ($j < 0$), the kinetically important reactant ions, tetrathionate and chlorite, migrate toward the boundary at $\zeta = +\infty$, whereas the autocatalyst hydrogen ion migrates in the opposite direction. This leads to a decrease in the overlap of the concentration fields for the reacting species resulting in a smaller integral for the reaction rate in eq 9. Hence, the velocity of propagation for planar fronts decreases as shown in Figure 4. A threshold field characterized with a constant current density ($j_{lim} = -20.72$) exists beyond which no sustained reaction front can be established and the system develops into a set of electrophoretic fronts moving independently of each other. In a positive field, where the reactants and the autocatalyst migrate toward each other, the increasing overlap of the reacting species results in a greater velocity of propagation.

The results of the two-dimensional calculations show that small perturbations within planar fronts decay and the planar symmetry is always sustained for negative electric field and in the absence of external electric field as shown in Figure 5a. Similarly to the experimental observations in positive external electric field, planar autocatalytic fronts become unstable at sufficiently high current density and cellular fronts with large amplitude develop (see Figure 5b).

The systematic investigation of stability reveals that upon increasing the current density, the dispersion curves of Figure 6 shift to greater values of the growth rate coefficients, which eventually leads to lateral instability with the appearance of positive ω for a range of wavenumbers. Since the bifurcation

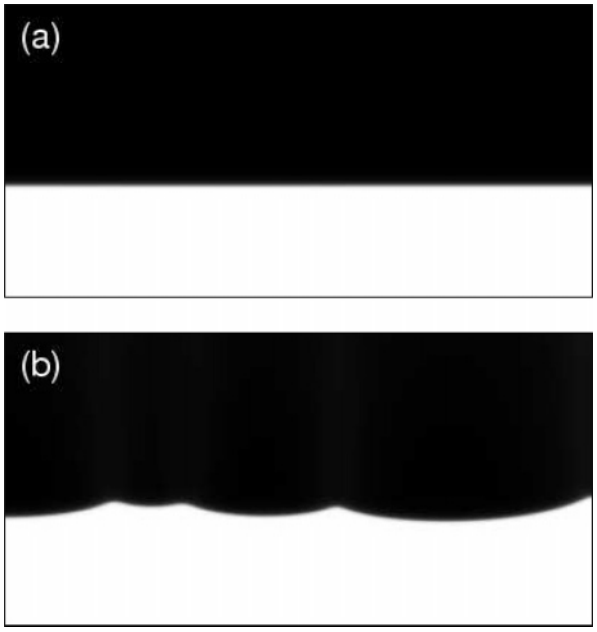

Figure 5. Gray scale representation of a calculated front at $j = 0.0$ (a) and $j = 20.0$ (b). Light regions correspond to low and dark regions to high concentration of the autocatalyst. Parameter value used for calculations: $\delta_3 = 2$.

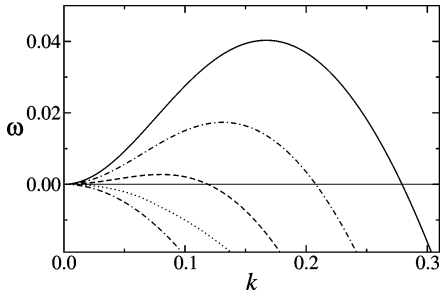

Figure 6. Dispersion curves of planar fronts calculated for $j = 0.0$, 2.0, 4.0, 6.0, and 8.0 from bottom up with $\delta_3 = 2$.

represents a long-wavelength instability, the onset of instability occurs when the gradient of the dispersion curve at the origin changes its sign from negative to positive as the current density increases. From the $d\omega/d(k^2)-j$ graph, constructed by fitting the function $\omega = Ak^2 - Bk^4$ to small wavenumbers of the dispersion curves and calculating the gradients at $k = 0$, the critical current density is given as $j_{cr} = 2.87$.

6. Discussion and Conclusion

The chlorite−tetrathionate reaction is an autocatalytic reaction with respect to the hydrogen ion, which diffuses significantly faster than other ions in aqueous solution. Greater diffusive flux of autocatalyst across the thin reaction front compared to that of reactants, however, leads to stabilized planar reaction−diffusion fronts in the absence of external electric field.[6] At first glance, an electric field oriented in the direction of front propagation with the negative electrode positioned ahead of the front would seem to further stabilize planar reaction fronts because of the following arguments. The imposed field introduces a migrational flux of the reactants and the autocatalyst toward each other which increases the local rate of reaction and hence the concentration of the autocatalyst in the back of the front. The latter, in turn, results in a greater diffusive flux with respect to that of the reactants further stabilizing the planar fronts.

The experiments clearly demonstrate that even though there is an enhanced mixing of the reactants and the autocatalyst in positive field, the greater velocity of propagation is a direct evidence of the increased local rate of reaction, planar fronts become unstable at a sufficiently strong field characterized by a critical current density. The lateral instability is governed by a range of small wavenumber modes that grow exponentially in time as shown by the experimental dispersion curves, since the wavenumber of the most unstable mode falls in the vicinity of the average wavelength of the observed cellular front in the initial stage of the pattern formation.

The source of instability arises from the stoichiometry of the reaction. There is a significant increase in ionic strength and mobility during the reaction as more ions are produced than consumed. As a result, the specific conductance of the product mixture becomes greater than that of the reactant mixture. In the experiments, we set a constant current density which can only be maintained if the potential gradient is greater ahead of the front than behind. It is therefore the enhanced migrational flux of the reactants that drives the instability in the positive field. The model based on the empirical rate law is able to exhibit the main features observed experimentally upon the introduction of an external electric field. In a negative field decreasing the current density, planar fronts remain stable up to a threshold beyond which the reaction fronts suddenly break up into independent electrophoretic fronts. In a positive field at a critical current density, planar fronts lose stability and cellular front emerge. The lateral instability is well characterized by the dispersion curves. The results of the calculations also support differential migration as the driving force of the instability arising from the difference in potential gradient on opposite sides of the thin reaction front. The semiquantitative agreement between the results of experiments and calculations can be best demonstrated by considering the following dimensional and dimensionless quantities: Figure 5 corresponds to 3.8 cm $\times$ 1.9 cm similar to Figure 2. The calculated onset of lateral instability is estimated at $J = 0.6$ mA/cm^2 representing the right order of magnitude for the experimentally determined value of $J_{cr} = 2.6$ mA/cm^2. For a better agreement, one has to resort to a more detailed kinetic model of the chlorite−tetrathionate reaction[22] and also take sodium hydroxide into account. The latter is present in the system to suppress selfinitiation and changes slightly the specific conductance of the solution by increasing it on the reactant side and decreasing on the product side of the reaction front.

The stabilizing effect of sodium hydroxide can also be demonstrated by adding sodium acetate to the solution. Sodium acetate slows down the diffusion rate of the autocatalyst hydrogen ion via the acetate−acetic acid equilibrium. The observed reaction fronts travel at smaller velocity of propagation in accordance with the decrease in the flux of the autocatalyst across the reaction front. Planar fronts, however, become more stable in the presence of sodium acetate and the critical current density for the onset of lateral instability slightly increases. The dispersion curves also lie below those obtained in the absence of sodium acetate in accordance with visual observations of the fronts. The addition of sodium acetate (or hydroxide) increases the ionic strength and hence the specific conductance of the reactant mixture, and by binding a fraction of the hydrogen ions produced, it decreases the specific conductance behind the reaction front. The overall difference in the magnitude of the migration flux of the reactants and the autocatalyst therefore shrinks representing a stabilizing step.

In conclusion, we have shown experimentally and theoretically that in reaction fronts of the autocatalytic chlorite−tetrathionate reaction, where the specific conductance increases in the course of the reaction, the selective enhancement of the migrational flux of the reactants with respect to that of the autocatalyst may alone lead to lateral instability. It is achieved with an external electric field oriented such a way that diffusional fluxes themselves have stabilizing nature in planar front. Migration driven instabilities using electric field, therefore, may be a more simple tool to produce cellular structures than applying selective immobilization for a reaction−diffusion front.

Acknowledgment. The initial experimental work of Tímea Evanyics is gratefully acknowledged. This work was supported by the Hungarian Scientific Research Fund (OTKA T046010).

References and Notes

(1) Epstein, I. R.; Showalter, K. *J. Phys. Chem.* **1996**, *100*, 13132.
(2) Epstein, I. R.; Pojman, J. A. *An Introduction to Nonlinear Dynamics: Oscillations, Waves, Patterns, and Chaos*; Oxford University Press: Oxford, 1998.
(3) van Saarloos, W. *Phys. Rep.* **2003**, *386*, 29.
(4) Kuramoto, Y. *Dynamics of Synergetic Systems*; Haken, H., Ed.; Springer: Berlin, 1980; p 134.
(5) Horváth, D.; Showalter, K. *J. Chem. Phys.* **1995**, *102*, 2471.
(6) Horváth, D.; Tóth, Á. *J. Chem. Phys.* **1998**, *108*, 1447.
(7) Tóth, Á.; Veisz, B.; Horváth, D. *J. Phys. Chem. A* **1998**, *102*, 5157.
(8) Davies, P. W.; Blanchedeau, P.; Dulos, E.; De Kepper, P. *J. Phys. Chem. A* **1998**, *102*, 8236.
(9) Horváth, D.; Petrov, V.; Scott, S. K.; Showalter, K. *J. Chem. Phys.* **1993**, *98*, 6332.
(10) Jakab, É.; Horváth, D.; Tóth, Á.; Merkin, J. H.; Scott, S. K. *Chem. Phys. Lett.* **2001**, *342*, 317.
(11) Tóth, Á.; Horváth, D.; Jakab, É.; Merkin, J. H.; Scott, S. K. *J. Chem. Phys.* **2001**, *114*, 9947.
(12) Horváth, D.; Tóth, Á.; Yoshikawa, K. *J. Chem. Phys.* **1999**, *111*, 10.
(13) Tóth, Á.; Horváth, D.; van Saarloos, W. *J. Chem. Phys.* **1999**, *111*, 10964.
(14) Merkin, J. H.; Kiss, I. Z. *Phys. Rev. E* **2005**, *72*, 026219.
(15) Virányi, Z.; Szommer, A.; Tóth, Á.; Horváth, D. *Phys. Chem. Chem. Phys.* **2004**, *9*, 3396.
(16) Ševčíková, H.; Marek, M.; Müller, S. C. *Science* **1992**, *257*, 951.
(17) Steinbock, O.; Schütze, J.; Müller, S. C. *Phys. Rev. Lett.* **1992**, *68*, 248.
(18) Schmidt, B.; De Kepper, P.; Müller, S. C. *Phys. Rev. Lett.* **2003**, *90*, 118302.
(19) Ševčíková, H.; Marek, M. *Physica D* **1984**, *13*, 379.
(20) Nagypál, I.; Epstein, I. R. *J. Phys. Chem.* **1981**, *90*, 6285.
(21) Tóth, Á.; Horváth, D.; Siska, A. *J. Chem. Soc., Faraday Trans.* **1997**, *93*, 73.
(22) Horváth, A. K. *J. Phys. Chem. A* **2005**, *109*, 5124.
(23) Fuentes, M.; Kuperman, M. N.; De Kepper, P. *J. Phys. Chem. A* **2001**, *105*, 6769.
(24) Boissonade, J.; Dulos, E.; Gauffre, F.; Kuperman, M. N.; De Kepper, P. *Faraday Discuss.* **2001**, *120*, 353.
(25) Gauffre, F.; Labrot, V.; Boissonade, J.; De Kepper, P.; Dulos, E. *J. Phys. Chem. A* **2003**, *107*, 4452.
(26) Virányi, Z.; Tóth, Á.; Horváth, D. *Chem. Phys. Lett.* **2005**, *401*, 575.
(27) Cohen, S. D.; Hindmarsh, A. C. *Comput. Phys.* **1996**, *10*, 138.
(28) Anderson, E.; et al. *LAPACK User's Guide*; Society for Industrial and Applied Mathematics: Philadelphia, 1999.